

Euler buckling in red blood cells: An optically driven biological micromotor

A. Ghosh^{a,b}, S. Sinha^{a,b}, J. A. Dharmadhikari^c, S. Roy^c, A. K.

Dharmadhikari^c, J. Samuel^b, S. Sharma^c, and D. Mathur^c

^aHarish Chandra Research Institute,

Chhatnag Road, Allahabad 211 019, India.

^bRaman Research Institute, Bangalore 560 080, India. and

^cTata Institute of Fundamental Research,

1 Homi Bhabha Road, Mumbai 400 005, India.

(Dated: February 9, 2020)

Abstract

We report the observation of an optically driven micromotor of biological origin. A single red blood cell (RBC) folds when placed in an optical trap. The folded RBC is birefringent and rotates in circularly polarized light. Optical forces permit a high degree of control over the speed and direction of rotation of such a micromotor. This cellular micromotor has potential applications in micromanipulation, possibly like an "optical screw driver" to apply torques at the micron scale. A simple theoretical model captures the main observed features and makes predictions that are successfully tested.

PACS numbers: 87.80.Cc, 87.80.Fe, 89.20.-a, 87.17.Aa

In a classical experiment Beth [1] demonstrated the conversion of optical energy into mechanical energy in a micron-sized quartz crystal that rotates in circularly polarized light. In the last few years there has been considerable interest in the design of miniature rotors as components of optically-driven micro-motor systems. Developments in nanotechnology place immediate needs for instrumentation to measure material properties such as, for example, the torsional elasticity of single proteins and DNA, and their microscopic viscosity [2]. Devices that are based on optical forces carry the obvious advantage that rotation can be caused without mechanical contact, so that an optically-driven micro-device may be rotated while in a sealed environment. Non-contact modes of rotation have been demonstrated in micro-motors [3, 4] involving specially shaped dielectrics and birefringent particles. Friese et al. [5] have demonstrated that optically-driven micro-machine elements are possible in principle by transferring angular momentum from circularly polarized light to a birefringent, photolithographically fabricated micro-structure with a resulting rotation speed as high as 350 Hz. Specially shaped rotors have been microfabricated by means of two-photon polymerization of light curing resins [4]. However, the stringent constraint on the shape and microfabrication of rotors continues to be a key challenge in hitherto existing work on light-driven micro-motors. Very recently, experiments have been reported in which the necessity for microfabrication of special shapes has been obviated by optical trapping of a naturally occurring material, biconcave disk-shaped red blood cells (RBCs) [6]. The rotation induced by optical forces can be finely controlled because it depends on controllable parameters like incident laser power and polarization state. One possible application of this effect is to use the rotating cell like an "optical screw driver" to apply torques at the micron scale. This would be useful for instance, in probing the torsional elasticity of biopolymers like DNA. It has been shown that conversion of optical energy into mechanical energy leads to rotation of trapped RBCs, yielding overall torques as high as 55,000 pN nm, a value that may be compared with typical torques of 40 pN nm that have been reported for molecular motors based on enzymatic action [8].

Experiments show that there is an initial step in the optically-induced process that involves a morphological change: the optical field first induces the biconcave disk to fold into a rod-like shape and it is this folded shape that rotates. The application of optical forces to naturally-occurring materials of cellular dimensions also holds much promise for new vistas in both basic research, like single cell molecular biology [9], and in applications like

laser-assisted in-vitro fertilization [7], cell biosensors [10], and new possibilities of micromanipulation, including cell sorting and construction of patterns for cellular microchips [10, 11]. However, there still remains a paucity of insight into the physics that governs the trapping of cellular level biological material. Although some initial insights have been developed on how imbalances in intracellular ionic concentrations may lead to anisotropies in polarizability [6], thereby generating optically-induced torques, the important physics of the precursor state involving the shape alteration of the trapped cell remains unaddressed. We seek to address this lacuna by presenting here the results of a combined experimental and theoretical study on the optically-induced folding of RBCs that enables a new level of understanding to be reached on the light-matter interaction that governs the overall dynamics.

Our optical trapping measurements on healthy RBCs were conducted using a single beam optical trap. A 1064 nm, 1 W diode pumped Nd:YVO₄ laser was used in conjunction with a 100X oil-immersed objective of large numerical aperture (NA = 1.3) to create a trap for micron-sized particles. Typical trapping forces of 2-10 pN were used. Blood samples from humans and mice were collected in a sterile anticoagulant containing glucose (136 mM), citric acid monohydrate (38.1 mM) and sodium citrate (74.8 mM) and centrifuged at 3000 rpm for 10 minutes. The plasma and buffy coat containing white blood cells was aspirated out and purified RBCs were washed with sterile RPMI medium containing 28 mM NaHCO₃, 25 mM HEPES and 80 g/ml gentamycin sulphate. The RBCs were resuspended in sterile RPMI medium containing 10% serum as a 50% suspension v/v and stored at 4°C. Before imaging RBCs were pelleted at 3000 rpm for 10 minutes, resuspended in PBS solution comprising of NaCl (136 mM), KCl (2.7 mM), Na₂HPO₄ (10.1 mM) and KH₂PO₄ with 2% BSA at a dilution of about 10⁶ cells/ml, from which 40-50 μ l was used on a microscope slide with a cover slip for imaging and trapping.

The normal RBC shape is a flattened biconcave disk; when an RBC is placed in an optical trap of sufficient strength, the compressive trap forces overcome the elasticity of the cell and fold it into a rod-like shape. Upon removal of the trap, the cells unfold into their original shape. Images that depict such deformation are shown in Fig. 1. The left column shows snapshots from a movie while the right column shows the folding in a cartoon format. The long axis of the folded RBC aligns itself along the laser polarization vector. Our measurements indicate that typical folding times (ca. 1s) are much smaller than unfolding times (ca. 14s). In the following we attempt to model these observations in a manner that

adequately captures the main experimental observations and make predictions that we are able to test.

We focus on the folding of RBCs. Neglecting its biconcave geometry, we take an RBC to be a flat, disc shaped elastic membrane with an energy cost for bending and deformation. The energy function for this elastic disc has two terms [12]: (i) The energy cost associated with the extrinsic curvature of the membrane,

$$E_c = B \int d^2 \mathbf{r} (\kappa)^2; \quad (1)$$

where $d^2 \mathbf{r}$ represents an area element on the membrane, B is the bending modulus and κ is the extrinsic curvature of the membrane and (ii) the energy cost of the strain internal to the membrane that is given by an integral over the membrane of the square of the strain tensor and is characterized by two elastic constants, the Lamé constants [13]. We assume that internal strains are prohibitively expensive and the internal geometry of the membrane is fixed. So, an untrapped RBC is a disc whose intrinsic and extrinsic curvatures are both zero. It is clear that the membrane can assume only shapes with zero intrinsic curvature because it takes far greater energy to change the intrinsic geometry. Apart from the elastic energy of the membrane there is also energy associated with the optical trap, and this is given by

$$E_{\text{trap}} = \frac{1}{2} \int d^2 \mathbf{r} \epsilon I(\mathbf{x}; \mathbf{y}; z); \quad (2)$$

where ϵ is the dielectric constant of the RBC and $I(\mathbf{x}; \mathbf{y}; z)$ is the local intensity of light, which provides an external potential in which the RBC sits. The higher the intensity, the lower is the potential $V(\mathbf{x}; \mathbf{y}; z) = \frac{1}{2} \epsilon I(\mathbf{x}; \mathbf{y}; z)$. We expand the potential in a Taylor series around the minimum of the potential (z is chosen along the direction of propagation of light),

$$V(\mathbf{x}; \mathbf{y}; z) = \frac{1}{2} A (x^2 + y^2) + \frac{1}{2} C z^2; \quad (3)$$

where A and C are constants proportional to the incident laser power. E_c is lowest when the RBC is flat and unfolded. E_{trap} is lowest when the RBC is at the bottom of the potential. The shape of the membrane is determined by a competition between E_c and E_{trap} . So, when the trap is switched on, for high enough laser power the folded state is more favorable, and when it is switched off the flat state is more favorable. This points to the fact that the trap stiffness wins over the membrane stiffness and thus the trap induces folding. The constraint

of preserving the intrinsic geometry of the membrane forces it to assume, as seen in Fig. 1, a rod-like shape rather than, for instance, a hemispherical shape. This is because a hemisphere has a non-zero intrinsic curvature unlike a cylinder. The allowed configurations of the elastic membrane in this model are similar to the allowed configurations of a disc made of paper: it can be bent into a cylinder, but not into a sphere as this deforms its internal geometry. An analysis of the two competing terms, the curvature energy and the trap energy shows that the threshold power needed for folding is inversely proportional to the cube of the linear dimension of the cell. This is a prediction of the model which can be tested against future experiments on this system.

We view the folding of the trapped RBC as an analog of the classical Euler buckling instability [13]: take an elastic rod (a ballpoint pen will do nicely) and compress it along its length. For small compressive forces, the rod remains straight. But at a critical value of the compressive force, the elastic rod buckles into a bent configuration. The buckling is a result of a competition between two energies, the energy associated with the force of compression, which tries to bend the rod and the elastic energy, which tries to keep it straight. Notice that although the RBC is modelled as a two dimensional disc, it bends only in one direction because of the constraint of preserving intrinsic geometry and so the problem is essentially one dimensional, just like the compressed rod. We can simplify the analysis even further by focussing on the lowest energy mode of deformation: one in which the RBC assumes a shape which is part of a cylinder of radius R . We may use as the order parameter the quantity $\alpha = d/R$, where d is the diameter of the RBC. $\alpha = 0$ corresponds to $R = d/2$, the unfolded state; a non-zero α describes a curved configuration. We would expect that the energy of bending is proportional to α^2 , since bending in either direction costs the same amount of energy. $E_c = a \alpha^2$, where a is a constant related to the bending modulus. Similarly, the trap energy is also symmetric in α and can be expressed as $E_{\text{trap}} = b \alpha^2$, where b is a constant related to the intensity of the laser radiation.

The time scales for folding and unfolding can also be understood in this simple model which has two parameters – the depth of the trap (experimentally controlled by the intensity of light) that is represented by b and the stiffness of the membrane represented by a . When α deviates from 0, it experiences a restoring force given by $F = (a - b) \alpha$. We note that all our experiments are conducted at low Reynolds number where viscous forces dominate over the negligible [14] inertial forces. As in any viscous medium, the force F causes a

motion whose velocity v is proportional to the applied force F ($v \propto F$). From this we conclude that the time scale for folding is given by $T_{\text{fold}} = 1/v = 1/(a - b)$, or in terms of the folding rate, $1/T_{\text{fold}} = P - P_0$, where P_0 is the critical laser power for folding. Since velocities are directly proportional to forces, time scales are inversely proportional to forces. The higher the force, the smaller the time scale. This picture explains why the folding time is much shorter than the unfolding time. The optical trap force induces folding and the process is fast. In contrast, when the trap is turned off, the membrane spontaneously and slowly relaxes back to its flat state as there are no forces on the membrane to keep it folded. Based on our model we expect that by controlling the intensity of the light beam one can change the folding time. As the laser power is lowered, the folding time is expected to increase and at a certain low power when the trap energy just cancels the elastic energy, we expect to see large fluctuations in the shape of the membrane. This is because at this power level there is no restoring force in the z variable. The membrane is floppy and susceptible to Brownian fluctuations. These large shape fluctuations have been experimentally seen. Figure 2 shows results of measurements of the dependence of the folding rate on normalized laser power; the results are in agreement with the predictions of our model.

It is also interesting to note that the folding corresponds to a broken symmetry. The RBC in the trap is subject to compressive forces, which are isotropic in the $x - y$ plane. Since the RBC has to fold along one direction, this direction is randomly picked out from all possible directions in the $x - y$ plane. We have explored what happens when we model the RBCs as elliptical objects. As indicated in Fig. 3, imagine the RBC as lying in the xy -plane, and we observe it along the z -direction. The optical forces act on the cell radially inwards and are exactly balanced. The buckling initiated by a random thermal kick can take place about an axis along L_1, L_2 , or in general along any arbitrary axis in the $x - y$ plane. Since, in general, folding occurs about any arbitrary axis one expects to see simultaneous changes in L_1 and L_2 . Measurements of L_1 and L_2 that we have made are shown in Fig. 3 and are, again, in agreement with the expectations of our model.

Having accounted for the folding behavior, we now consider the rotation of a trapped RBC. To compute the light forces on the RBC we have used classical electromagnetic theory to express the force and torque on the cell as integrals of bilinears of the electromagnetic field over the cell. However, an equivalent but more intuitive way is to think in terms of photons: each photon which is incident on the cell has momentum p_i and spin S_i . When

this photon leaves the cell it carries momentum p_f and spin S_f , since both its direction and state of polarization may have changed. We can then compute the forces and torques on the cell by using momentum and angular momentum conservation. Each photon produces a "recoil" momentum and angular momentum. Multiplying this by the number of photons per second we find the forces and torques that are generated on the RBC. The final answer can, of course, be expressed purely in terms of classical notions like laser power, frequency and polarization. The momentum p carried by a photon is $h\mathbf{k}$, where \mathbf{k} is the wave vector. The "spin" or polarization is best described using the Poincare Sphere. For a photon, whose spin is $1\hbar$, the north pole ($\theta = 0$) represents right circularly polarized light with angular momentum \hbar and the south pole ($\theta = 180^\circ$) represents left circularly polarized light, with angular momentum of $-\hbar$. Linearly polarized light carries no spin angular momentum and is represented along the equator while all other points on the sphere represent elliptically polarized light. In passing through the RBC, which is birefringent, the state of polarization of the incident photon changes from circular to elliptical. The difference in spin angular momentum is imparted to the RBC, thus exerting a torque on the RBC causing it to rotate. The change in angular momentum is proportional to the change in $\cos\theta$, and therefore to the change in the z -coordinate of the Poincare Sphere, multiplied by the unit of angular momentum. One can express the torque as $\tau = N\hbar\Delta z$, where Δz is a dimensionless number, the change in the z -coordinate on the Poincare sphere and N is the number of photons per second. By multiplying and dividing by ω , the frequency of the radiation, we obtain the purely classical formula for the torque $\tau = P/\omega$, where P is the power of the incident laser light, which is the number of photons per second multiplied by the energy $h\omega$ of each photon. We, therefore, expect the torque that is generated to be proportional to the incident laser power. This is indeed what is observed in the measurements that we show in Fig. 4.

To summarize, we address the physics that governs the two stages leading to optically-induced micromotor action of a red blood cell in an optical trap. The first stage involves a morphological change that makes use of the elasticity of the biomembrane; the second stage involves micromanipulation of the folded cell using light forces. A theoretical model that uses the concept of Euler instability is successfully employed to rationalize the cell folding that is observed. We expect this work to generate interest amongst biologists and physicists to explore new avenues in this emerging area of optically-driven biological micromotors. We expect this integration into the physics of cellular dynamics of a treatment of instabilities

that has hitherto been of considerable utility in polymer physics, soft condensed matter physics, and mechanical engineering might also assume importance in forthcoming developments in the interdisciplinary area of optically-driven biological micromotors and membrane dynamics.

-
- [1] R. A. Beth, *Phys. Rev.* 50, 115 (1936).
 - [2] C. Bustamante, Z. Bryant, and S. B. Smith, *Nature* 421, 423 (2003).
 - [3] E. Higurashi, O. Ohguchi, T. Tamamura, H. Ukita, and R. Sawada, *J. Appl. Phys.* 82, 2773 (1997).
 - [4] P. Galajda and P. Oromos, *Appl. Phys. Lett.* 78, 249 (2001).
 - [5] M. E. J. Friese, H. Rubinsztein-Dunlop, J. Gold, P. Hagberg, and D. Hanstorp, *Appl. Phys. Lett.* 78, 547 (2001).
 - [6] J. A. Dhamadhikari, S. Roy, A. K. Dhamadhikari, S. Sharma, and D. Mathur, *Opt. Express* 12, 1179 (2004).
 - [7] M. Zahn and S. Seeger, *Cell. Mol. Biol.* 44, 747 (1998).
 - [8] K. Kinoshita Jr., R. Yasuda, H. Noji, and K. Adachi, *Phil. Trans. Roy. Soc. London B* 355, 473 (2000).
 - [9] K. Schutze, G. Posl, and G. Lahr, *Cell. Mol. Biol.* 44, 735 (1998).
 - [10] A. Clement-Sengewald, K. Schutze, A. Ashkin, G. A. Palma, G. Kerken, and G. Brenner, *J. Assisted Reproduction Genetics* 13, 259 (1996).
 - [11] M. Zahn, J. Renken, and S. Seeger, *FEBS Letters* 443, 337 (1999).
 - [12] Y. Kantor and D. R. Nelson, *Phys. Rev. Lett.* 58, 2774 (1987).
 - [13] L. D. Landau and E. M. Lifshitz, *Theory of Elasticity*, Pergamon Press, NY, 1986.
 - [14] H. C. Berg, *Random Walks In Biology*, Princeton University Press, Princeton, 1993.

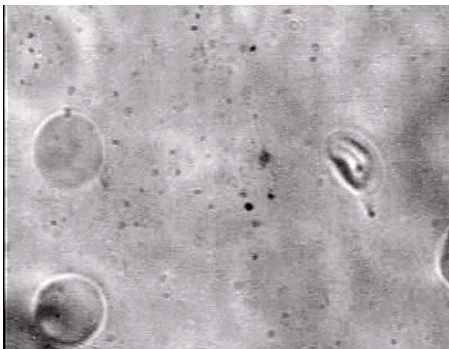
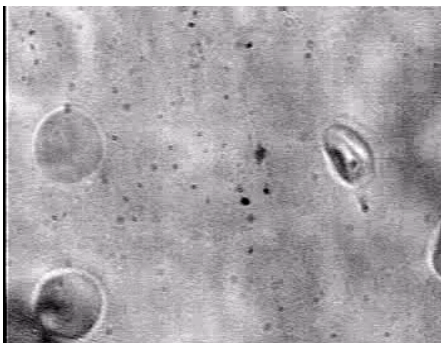
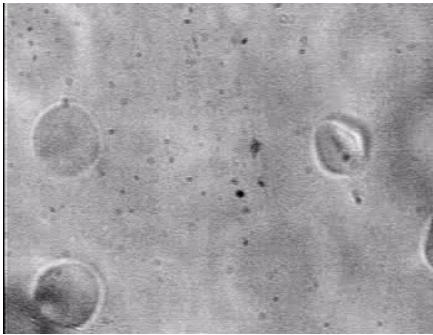
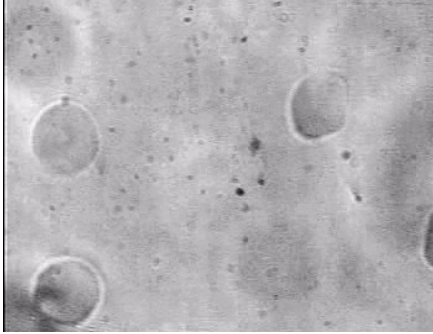
FIG . 1: On placing a biconcave, disk-like red blood cell in an optical trap, it undergoes folding that is depicted in (a) frames from a real-time movie and (b) in cartoon form at. Each movie frame is taken 250 ms after the preceding one. Upon removal of the trap, unfolding occurs over a typical time scale of ca. 14s.

FIG . 2: Dependence of folding rate on normalized laser power, P/P_0 , where P is the incident laser power and P_0 is the power below which folding does not occur for a 6 μ m RBC .

FIG . 4: Variation of the torque generated in a rotating RBC with incident laser power, using circularly polarized light.

FIG . 3: Variation of the RBC dimensions, L_1 and L_2 , with folding time.

(a)



(b)

